

# Valence-Band Tunneling Enhanced Hot Carrier Degradation in Ultra-Thin Oxide nMOSFETs

C.W. Tsai, S.H. Gu, L.P. Chiang, Tahui Wang,  
Department of Electronics Engineering, National Chiao-Tung University, Taiwan  
Y.C. Liu, L.S. Huang,, M.C. Wang and L.C. Hsia  
Technology and Process Development Division, UMC, Hsin-Chu, Taiwan

## Abstract

Enhanced hot carrier degradation with stress  $V_g$  in the valence-band tunneling regime is observed. This degradation is attributed to channel hole creation by valence-band electron tunneling. The created holes provide for Auger recombination with electrons in the channel and thus increase hot electron energy. The valence-band tunneling enhanced hot carrier degradation becomes more serious as gate oxide thickness is reduced. In ultra-thin gate oxide nMOSFETs, our result shows that the valence-band tunneling enhanced degradation, as opposed to max.  $I_b$  stress induced degradation, exhibits positive dependence on substrate bias. This phenomenon may cause a severe reliability issue in positively biased substrate or floating substrate devices.

## Introduction

It has been reported that Auger recombination can enhance hot electron tail and cause more serious degradation in MOSFETs [1-3]. The process for Auger recombination in various device structures and operation conditions is illustrated in Fig. 1. In Fig. 1(a), holes created by impact ionization flow to the region near the source (where electron concentration is high) in a SOI structure [4] and provide for recombination with electrons. In Fig. 1(b), a positive substrate bias is applied in a nMOSFET. As a result of substrate hole injection, the channel hole concentration and thus Auger recombination rate are enhanced [3]. In ultra-thin oxide nMOSFETs, a positive gate bias can cause valence-band electron direct tunneling to the gate and leave holes behind in the channel for Auger recombination (Fig. 1(c)). In this work, it is our intention to investigate the significance of these valence-band tunneling created holes to device reliability.

Ultra-thin oxide nMOSFETs with gate oxide thickness from 17Å to 33Å are used in this work. The devices have a gate width of 10µm. Hot carrier stress with different stress  $V_g$  is performed. Drain current degradation is measured in the triode region at  $V_d=0.1V$  and  $V_g=1.5V$ . Stress time is 500sec.

## Results and Discussion

It has been shown in literature that in short channel devices hot carrier degradation at  $V_g=V_d$  stress is more serious than at max.  $I_b$  stress ( $V_g\sim 0.5V_d$ ) [5,6]. Fig. 2(a) shows the drain current degradation in two different gate-length nMOSFETs,  $L_g=0.20\mu m$  and  $L_g=0.13\mu m$ . The oxide thickness is  $t_{ox}=25\text{Å}$ . The corresponding  $I_b$  in stress is plotted in Fig. 2(b). In the 0.2µm device, the worst stress condition occurs around max.  $I_b$  while in the 0.13µm device the degradation increases monotonically with  $V_g$ . This behavior was explained in [6] because (i) the  $I_b$ - $V_g$  curve is relatively flat in the 0.13µm device and (ii) channel hot electrons are confined more closely to the Si surface, thus leading to larger damage to the Si surface, at a larger  $V_g$ .

Notably, as stress  $V_g$  increases above 3V, a drastic rise of the degradation is observed in both devices. The subthreshold characteristics at a low  $V_g$  stress and at a high  $V_g$  stress are shown in Fig. 3. The swing degradation indicates interface trap creation by the two stresses. The stress time dependence of the drain current degradation in Fig. 4 also confirms that the degradations at a low  $V_g$  stress and at a high  $V_g$  stress are both due to interface trap creation.

To investigate the correlation between the drastic rise of the degradation and valence band tunneling, we measured  $I_d$  degradation and valence-band tunneling current in nMOSFETs with different  $t_{ox}$  (Fig. 5). The  $t_{ox}=33\text{Å}$  device has a gate length of 0.16µm and other devices have a gate length of 0.13µm. The substrate current measured at  $V_d=0V$ , which reflecting valence-band tunneling, is shown in Fig. 5(b). The following features should be noted. First, the rise of the  $I_d$  degradation in the valence-band tunneling regime is observed in all the devices except for the  $t_{ox}=33\text{Å}$  device. The valence-band tunneling current in the 33Å device is found to be negligible (result not shown in Fig. 5(b)). Secondly, the degradation at max.  $I_b$  stress decreases when  $t_{ox}$  reduces. This part is in agreement with the findings by Momose [7] that thinner oxides have better hot carrier reliability. However, an opposite trend (i.e., the degradation increases as  $t_{ox}$  reduces) is found when the devices are stressed in the valence-band tunneling regime. The process for valence-band tunneling enhanced hot carrier stress is proposed in Fig. 6. In Fig. 6(a), channel holes are created due to valence-band electron tunneling. The generated holes then provide for recombination with electrons in the channel

and transfer the excess energy to other conduction electrons (Fig. 6(b)). The energetic electrons arising from the Auger process are subsequently accelerated by a lateral electric field near the drain (Fig. 6(c)), thus resulting in a larger hot electron tail and higher interface trap generation rate. The entire electron energy gain process therefore depends on  $V_g$  (valence band tunneling) and  $V_d$  (lateral field acceleration).

To further verify the role of valence-band tunneling created holes in the degradation, we change the substrate bias in stress (Fig. 7) to modulate the hole concentration in the channel. Fig. 8 shows the variation of  $I_g$  and  $I_b$  with substrate bias in the low  $V_g$  and high  $V_g$  stresses. For  $t_{ox}=20\text{\AA}$  devices (Fig. 7(a)), the degradation in the low  $V_g$  region and in the high  $V_g$  region exhibits opposite substrate bias dependence. The simulated lateral electric field distribution and the conduction band-edge diagram in the vertical direction are plotted in Fig. 9. As  $V_b$  changes from 0V to -1V, the peak lateral channel field slightly increases (Fig. 9(a)), implying stronger lateral field heating. Moreover, the vertical field is also increased, which means the channel electrons are pushed further toward the  $S_i$  surface (Fig. 9(b)). These two factors lead to a larger gate current (Fig. 8) and increased  $I_d$  degradation in the low  $V_g$  region. In the high  $V_g$  region, we have shown valence-band tunneling plays an important role in the degradation. A negative substrate bias can help remove the channel holes to the substrate and thus reduce the hole effect. As a result, the  $I_d$  degradation becomes smaller at a negative substrate bias although the stress gate current and substrate current are larger (Fig. 8). This result actually excludes the possibility that the rise of the  $I_d$  degradation at a large  $V_g$  is primarily caused by the increase of stress  $I_g$ .

In contrast, the  $t_{ox}=33\text{\AA}$  device shows negative substrate bias dependence in the entire range of stress  $V_g$  because of negligible valence-band tunneling effect. In Fig. 10, we plot the  $I_d$  degradation versus the substrate bias in stress. The stress gate bias is 1.3V (max.  $I_b$  stress) for the lower curve and 3.4V (valence-band tunneling stress) for the upper curve. The valence-band tunneling enhanced degradation, as opposed to max.  $I_b$  stress induced degradation, shows positive dependence on substrate bias and may impose a constraint in the DTMOS-like operation [8]. The degradation in a floating substrate stress condition is also indicated in the figure.

### Conclusion

The significance of valence-band tunneling to hot carrier degradation in ultra-thin oxide MOSFETs has been evaluated. The valence-band tunneling enhanced degradation becomes more severe as the gate oxide thickness is reduced. Our study shows this degradation mode exhibits positive substrate bias dependence and may appear to be a new reliability issue in certain applications, such as floating substrate devices (SOI) or positively biased substrate devices (DTMOS).

### Acknowledgements

The authors would like to acknowledge financial support from NSC, Taiwan (NSC 89-2215-E009-034) and from UMC, Taiwan (89C189).

### References

- [1] B. Ricco, E. Sangiorgi, and D. Cantarelli, "Low voltage hot-electron effects in short channel MOSFETs", IEEE International Electron Devices Meeting, p. 92, 1984.
- [2] R. Shirota and T. Yamaguchi, "A new analytical model for low voltage hot electron taking Auger recombination as well as phonon scattering process into account", IEEE International Electron Devices Meeting, p. 123, 1991.
- [3] L. P. Chiang, C. W. Tsai and T. Wang, "Auger recombination enhanced hot carrier degradation in nMOSFETs with positive substrate bias", in Symp. VLSI Tech. Dig., p. 132, 2000.
- [4] M. Yamaji, K. Taniguchi, C. Hamaguchi, K. Sukegawa and S. Kawamura, "Degradation mechanisms of thin film SIMOX SOI-MOSFET characteristics optical and electrical evaluation", IEICE Trans. Electron., vol. E77-C, 1994.
- [5] L. Su, et al., "A high-performance 0.08 $\mu\text{m}$  CMOS", in Symp. VLSI Tech. Deg., p. 12, 1996.
- [6] E. Li, E. Rosenbaum, J. Tao, G. C. F. Yeap, M. R. Lin and P. Fang, "Hot carrier effects in nMOSFETs in 0.1 $\mu\text{m}$  CMOS technology", in Proc. IEEE Reliab. Phys. Symp. p. 253, 1999.
- [7] H. S. Momose, S. Nakamura, T. Ohguro, T. Yoshitomi, E. Morifuji, T. Morimoto, Y. Katsumata and H. Iwai, "A study of hot-carrier degradation in n and p-MOSFETs with ultra-thin gate oxides in the direct-tunneling regime", IEEE International Electron Devices Meeting, p. 453, 1997.
- [8] F. Assaderaghi, D. Sinititsky, S. Parke, J. Boker, P. K. Ko and C. Hu, "A dynamic threshold voltage MOSFET (DTMOS) for ultra-low voltage operation", IEEE International Electron Devices Meeting, p. 809, 1994.

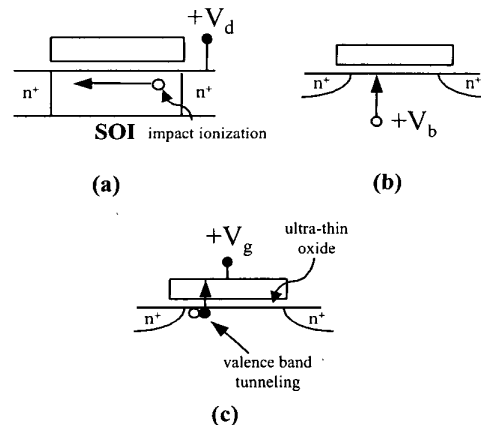


Fig.1 Auger recombination process in various nMOSFET structures and operation conditions.  
 (a) Impact ionization created holes flowing to the region near the source in a SOI MOSFET[4].  
 (b) Substrate hole injection to the channel by a positive substrate bias in DTMOS operation [3].  
 (c)  $+V_g$  induced valence-band electron tunneling in ultra-thin oxide nMOSFETs and leaving holes in Si substrate.

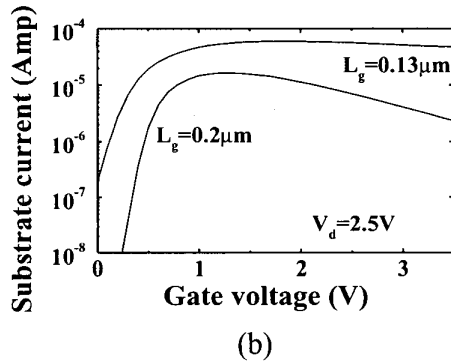
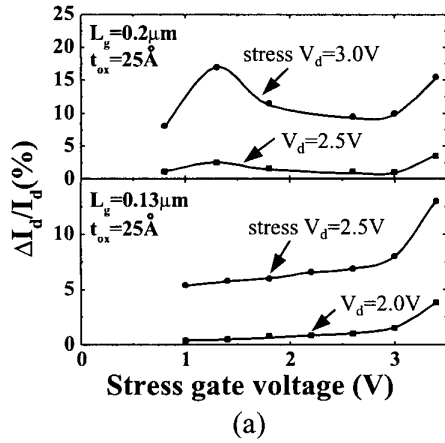


Fig.2(a)  $I_d$  degradation versus stress gate bias in  $L_g=0.20\mu\text{m}$  and  $L_g=0.13\mu\text{m}$  nMOSFETs. Stress  $V_d$  is 3.0V, 2.5V and 2.0V. Stress time is 500 sec.  $I_d$  degradation is measured at  $V_d=0.1\text{V}$  and  $V_g=1.5\text{V}$ . (b) Substrate current versus gate voltage,  $V_d=2.5\text{V}$ .

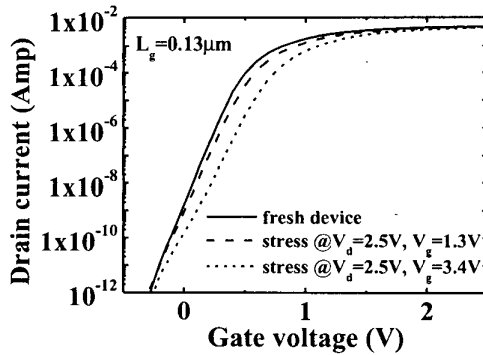


Fig.3 Measured subthreshold characteristics in a fresh device, after  $V_d=2.5\text{V}$  and  $V_g=1.3\text{V}$  stress and after  $V_d=2.5\text{V}$  and  $V_g=3.4\text{V}$  stress. Stress time is 500 sec. The swing degradation indicates that the cause of degradation is interface trap creation.

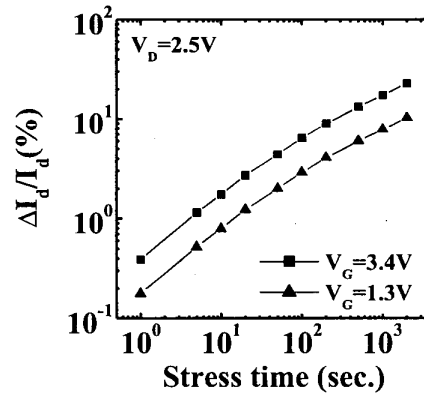


Fig.4  $I_d$  degradation versus stress time in devices stressed at  $V_g=1.3\text{V}$  and  $V_g=3.4\text{V}$ . Stress drain bias is 2.5V. The power factor is about 0.4, which reflects the growth rate of interface traps.

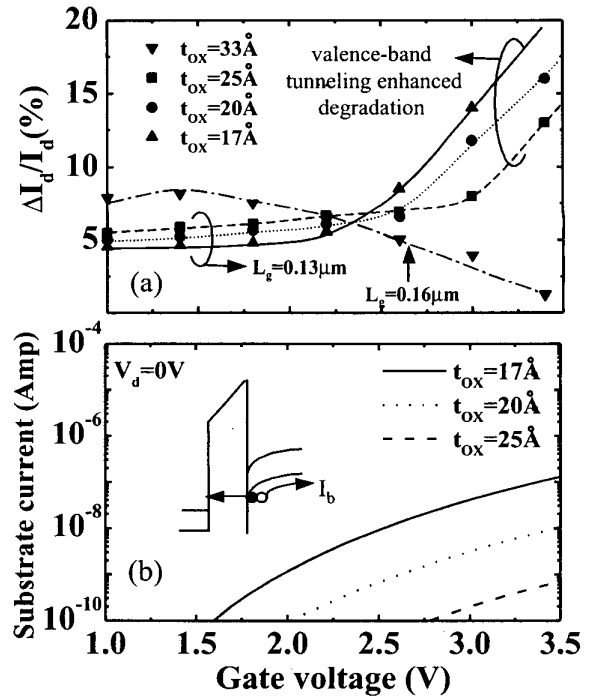


Fig.5 (a)  $I_d$  degradation versus stress gate bias in nMOSFETs with  $t_{\text{ox}}=17\text{Å}$ , 20Å, 25Å and 33Å. Stress  $V_d$  is 3.0V for the  $t_{\text{ox}}=33\text{Å}$  device and 2.5V for other devices. (b) Substrate current versus gate bias with  $V_d=0\text{V}$ . This substrate current results from valence-band electron tunneling. The valence-band tunneling current in the 33Å device is found to be negligible.

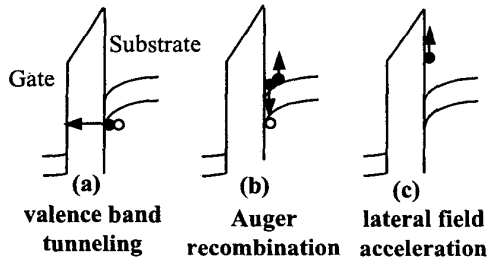


Fig. 6 Illustration of valence-band tunneling enhanced hot electron process.

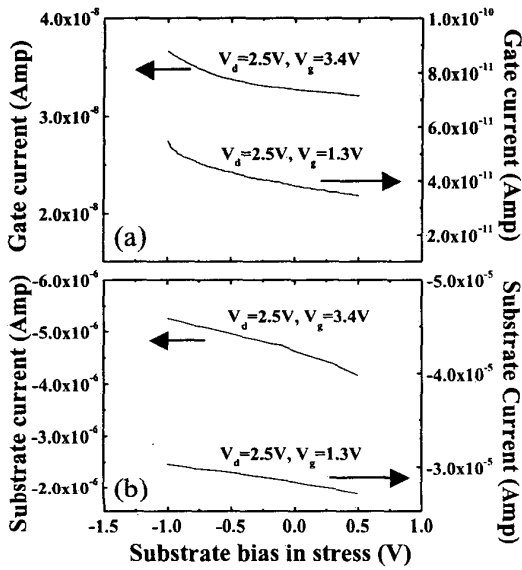


Fig. 8 Dependence of gate current and substrate current on substrate bias in stress.  $L_g = 0.13\mu\text{m}$  and  $t_{\text{ox}} = 25\text{\AA}$ .

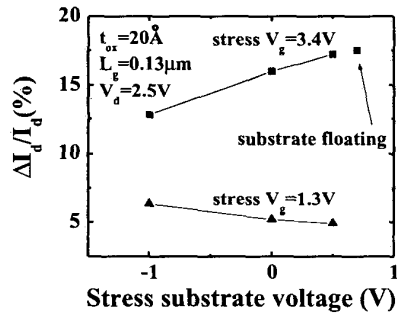


Fig. 10 Substrate bias dependence of the drain current degradation at two different stress  $V_g$ , 1.3V and 3.4V. The degradation in a stress condition of  $V_d = 2.5\text{V}$ ,  $V_g = 3.4\text{V}$  and substrate floating is indicated.

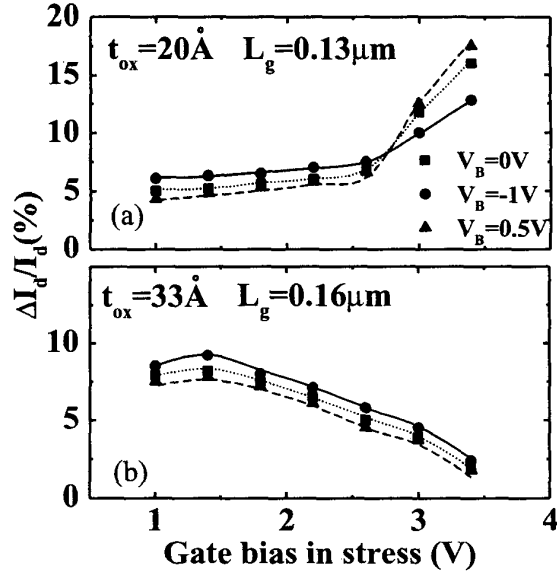
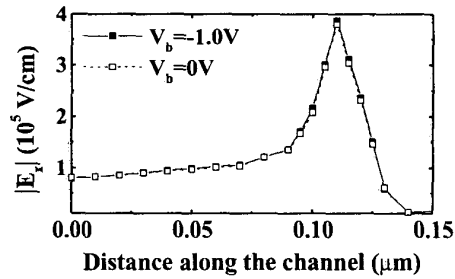
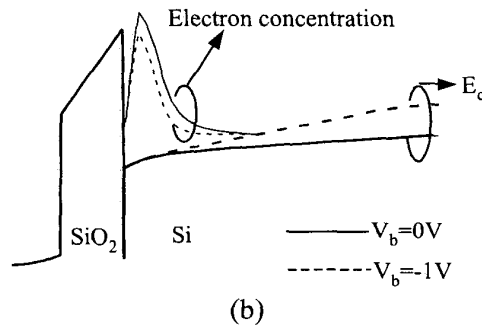


Fig. 7 Drain current degradation with different substrate bias in stress,  $V_B = 0.5\text{V}$ ,  $0\text{V}$  and  $-1\text{V}$ . (a)  $t_{\text{ox}} = 20\text{\AA}$  and stress  $V_d = 2.5\text{V}$ . (b)  $t_{\text{ox}} = 33\text{\AA}$  and stress  $V_d = 3.0\text{V}$ .



(a)



(b)

Fig. 9(a) Simulated lateral field distributions along the channel.  $V_d = 2.5\text{V}$ ,  $V_g = 3.4\text{V}$ ,  $V_b = 0\text{V}$  and  $-1\text{V}$ . The source junction is at  $x = 0.0\mu\text{m}$ . (b) Simulated conduction band-edge diagram and electron concentration distribution in the vertical direction from coupled 1D Poisson equation and Schrodinger equation. The centroid of the electron distribution is closer to the Si surface at  $V_b = -1\text{V}$ .

## 6.6.4